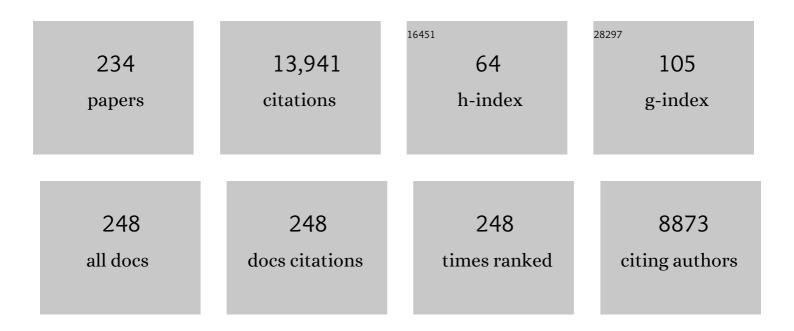
List of Publications by Year in descending order

Source: https://exaly.com/author-pdf/4570674/publications.pdf Version: 2024-02-01



#	Article	lF	CITATIONS
1	Review on the criteria anticipated for the fabrication of highly efficient ZnO-based visible-light-driven photocatalysts. Journal of Industrial and Engineering Chemistry, 2018, 62, 1-25.	5.8	697
2	Magnetically separable nanocomposites based on ZnO and their applications in photocatalytic processes: A review. Critical Reviews in Environmental Science and Technology, 2018, 48, 806-857.	12.8	464
3	Review on magnetically separable graphitic carbon nitride-based nanocomposites as promising visible-light-driven photocatalysts. Journal of Materials Science: Materials in Electronics, 2018, 29, 1719-1747.	2.2	462
4	Review on photocatalytic conversion of carbon dioxide to value-added compounds and renewable fuels by graphitic carbon nitride-based photocatalysts. Catalysis Reviews - Science and Engineering, 2019, 61, 595-628.	12.9	452
5	Review on heterogeneous photocatalytic disinfection of waterborne, airborne, and foodborne viruses: Can we win against pathogenic viruses?. Journal of Colloid and Interface Science, 2020, 580, 503-514.	9.4	412
6	Fabrication of novel magnetically separable nanocomposites using graphitic carbon nitride, silver phosphate and silver chloride and their applications in photocatalytic removal of different pollutants using visible-light irradiation. Journal of Colloid and Interface Science, 2016, 480, 218-231.	9.4	381
7	g-C3N4/carbon dot-based nanocomposites serve as efficacious photocatalysts for environmental purification and energy generation: A review. Journal of Cleaner Production, 2020, 276, 124319.	9.3	379
8	Ultrasonic-assisted preparation of plasmonic ZnO/Ag/Ag2WO4 nanocomposites with high visible-light photocatalytic performance for degradation of organic pollutants. Journal of Colloid and Interface Science, 2017, 491, 216-229.	9.4	271
9	Magnetically separable ternary g-C3N4/Fe3O4/BiOI nanocomposites: Novel visible-light-driven photocatalysts based on graphitic carbon nitride. Journal of Colloid and Interface Science, 2016, 465, 83-92.	9.4	258
10	Graphitic carbon nitride-based photocatalysts: Toward efficient organic transformation for value-added chemicals production. Molecular Catalysis, 2020, 488, 110902.	2.0	245
11	Nitrogen photofixation ability of g-C3N4 nanosheets/Bi2MoO6 heterojunction photocatalyst under visible-light illumination. Journal of Colloid and Interface Science, 2020, 563, 81-91.	9.4	166
12	Application of AlMCM-41 for competitive adsorption of methylene blue and rhodamine B: Thermodynamic and kinetic studies. Journal of Hazardous Materials, 2010, 178, 349-355.	12.4	162
13	Novel ternary g -C 3 N 4 /Fe 3 O 4 /Ag 2 CrO 4 nanocomposites: magnetically separable and visible-light-driven photocatalysts for degradation of water pollutants. Journal of Molecular Catalysis A, 2016, 415, 122-130.	4.8	155
14	Graphitic carbon nitride nanosheets decorated with CuCr2O4 nanoparticles: Novel photocatalysts with high performances in visible light degradation of water pollutants. Journal of Colloid and Interface Science, 2017, 504, 697-710.	9.4	150
15	Simultaneous Dual-Functional Photocatalysis by g-C ₃ N ₄ -Based Nanostructures. ACS ES&T Engineering, 2022, 2, 564-585.	7.6	149
16	Boosting visible-light photocatalytic performance of g-C3N4/Fe3O4 anchored with CoMoO4 nanoparticles: Novel magnetically recoverable photocatalysts. Journal of Photochemistry and Photobiology A: Chemistry, 2019, 368, 120-136.	3.9	143
17	Novel magnetic Fe 3 O 4 /ZnO/NiWO 4 nanocomposites: Enhanced visible-light photocatalytic performance through p-n heterojunctions. Separation and Purification Technology, 2017, 184, 334-346.	7.9	132
18	Decoration of carbon dots and AgCl over g-C3N4 nanosheets: Novel photocatalysts with substantially improved activity under visible light. Separation and Purification Technology, 2018, 199, 64-77	7.9	126

#	Article	IF	CITATIONS
19	Simple and large scale refluxing method for preparation of Ce-doped ZnO nanostructures as highly efficient photocatalyst. Applied Surface Science, 2013, 265, 591-596.	6.1	121
20	Fine cutting edge shaped Bi2O3rods/reduced graphene oxide (RGO) composite for supercapacitor and visible-light photocatalytic applications. Journal of Colloid and Interface Science, 2017, 498, 449-459.	9.4	121
21	Graphitic carbon nitride nanosheets coupled with carbon dots and BiOI nanoparticles: Boosting visible-light-driven photocatalytic activity. Journal of the Taiwan Institute of Chemical Engineers, 2018, 87, 98-111.	5.3	118
22	Ternary g-C3N4/ZnO/AgCl nanocomposites: Synergistic collaboration on visible-light-driven activity in photodegradation of an organic pollutant. Applied Surface Science, 2015, 358, 261-269.	6.1	117
23	Ternary TiO2/Fe3O4/CoWO4 nanocomposites: Novel magnetic visible-light-driven photocatalysts with substantially enhanced activity through p-n heterojunction. Journal of Colloid and Interface Science, 2018, 524, 325-336.	9.4	114
24	Decoration of carbon dots over hydrogen peroxide treated graphitic carbon nitride: Exceptional photocatalytic performance in removal of different contaminants under visible light. Journal of Photochemistry and Photobiology A: Chemistry, 2019, 374, 161-172.	3.9	113
25	Fe3O4/ZnO/CoWO4 nanocomposites: Novel magnetically separable visible-light-driven photocatalysts with enhanced activity in degradation of different dye pollutants. Ceramics International, 2017, 43, 3063-3071.	4.8	112
26	Magnetically recoverable highly efficient visible-light-active g-C3N4/Fe3O4/Ag2WO4/AgBr nanocomposites for photocatalytic degradations of environmental pollutants. Advanced Powder Technology, 2018, 29, 94-105.	4.1	111
27	Review on the hazardous applications and photodegradation mechanisms of chlorophenols over different photocatalysts. Environmental Research, 2021, 195, 110742.	7.5	111
28	Visible-light-induced nitrogen photofixation ability of g-C3N4 nanosheets decorated with MgO nanoparticles. Journal of Industrial and Engineering Chemistry, 2020, 84, 185-195.	5.8	105
29	Facile synthesis of novel CaFe 2 O 4 /g-C 3 N 4 nanocomposites for degradation of methylene blue under visible-light irradiation. Journal of Colloid and Interface Science, 2016, 480, 126-136.	9.4	104
30	Fabrication of novel magnetically separable visible-light-driven photocatalysts through photosensitization of Fe 3 O 4 /ZnO with CuWO 4. Journal of Industrial and Engineering Chemistry, 2016, 44, 174-184.	5.8	101
31	A comprehensive study on antidiabetic and antibacterial activities of ZnO nanoparticles biosynthesized using Silybum marianum L seed extract. Materials Science and Engineering C, 2019, 97, 397-405.	7.3	100
32	Deposition of CuWO 4 nanoparticles over g-C 3 N 4 /Fe 3 O 4 nanocomposite: Novel magnetic photocatalysts with drastically enhanced performance under visible-light. Advanced Powder Technology, 2018, 29, 1379-1392.	4.1	97
33	Novel magnetically separable ZnO/AgBr/Fe ₃ O ₄ /Ag ₃ VO ₄ nanocomposites with tandem n–n heterojunctions as highly efficient visible-light-driven photocatalysts. RSC Advances, 2016. 6. 2402-2413.	3.6	95
34	Novel TiO 2 /Ag 2 CrO 4 nanocomposites: Efficient visible-light-driven photocatalysts with n–n heterojunctions. Journal of Photochemistry and Photobiology A: Chemistry, 2017, 341, 57-68.	3.9	95
35	g-C3N4 nanosheets decorated with carbon dots and CdS nanoparticles: Novel nanocomposites with excellent nitrogen photofixation ability under simulated solar irradiation. Ceramics International, 2019, 45, 2542-2555.	4.8	95
36	Titania-activated persulfate for environmental remediation: the-state-of-the-art. Catalysis Reviews - Science and Engineering, 2023, 65, 118-173.	12.9	94

#	Article	IF	CITATIONS
37	ZnO/NiWO4/Ag2CrO4 nanocomposites with p-n-n heterojunctions: highly improved activity for degradations of water contaminants under visible light. Separation and Purification Technology, 2018, 193, 69-80.	7.9	90
38	Facile fabrication of novel ZnO/CoMoO 4 nanocomposites: Highly efficient visible-light-responsive photocatalysts in degradations of different contaminants. Journal of Photochemistry and Photobiology A: Chemistry, 2018, 363, 31-43.	3.9	89
39	Perovskite-type lanthanum ferrite based photocatalysts: Preparation, properties, and applications. Journal of Energy Chemistry, 2022, 66, 314-338.	12.9	88
40	Activation of persulfate by novel TiO2/FeOCl photocatalyst under visible light: Facile synthesis and high photocatalytic performance. Separation and Purification Technology, 2020, 250, 117268.	7.9	85
41	Solvatochromic Parameters for Binary Mixtures of 1-(1-Butyl)-3-methylimidazolium Tetrafluoroborate with Some Protic Molecular Solvents. Journal of Physical Chemistry B, 2006, 110, 7073-7078.	2.6	84
42	Simple and large scale one-pot method for preparation of AgBr–ZnO nanocomposites as highly efficient visible light photocatalyst. Applied Surface Science, 2013, 283, 1080-1088.	6.1	84
43	Photosensitization of ZnO by AgBr and Ag2CO3: Nanocomposites with tandem n-n heterojunctions and highly enhanced visible-light photocatalytic activity. Journal of Colloid and Interface Science, 2016, 474, 103-113.	9.4	84
44	BiOBr and AgBr co-modified ZnO photocatalyst: A novel nanocomposite with p-n-n heterojunctions for highly effective photocatalytic removal of organic contaminants. Journal of Photochemistry and Photobiology A: Chemistry, 2019, 379, 11-23.	3.9	82
45	Novel gâ€C ₃ N ₄ nanosheets/CDs/BiOCl photocatalysts with exceptional activity under visible light. Journal of the American Ceramic Society, 2019, 102, 1435-1453.	3.8	81
46	Novel magnetically separable g-C3N4/AgBr/Fe3O4 nanocomposites as visible-light-driven photocatalysts with highly enhanced activities. Ceramics International, 2015, 41, 5634-5643.	4.8	80
47	Novel ternary g-C 3 N 4 /Fe 3 O 4 /MnWO 4 nanocomposites: Synthesis, characterization, and visible-light photocatalytic performance for environmental purposes. Journal of Materials Science and Technology, 2018, 34, 1638-1651.	10.7	80
48	Novel ZnO/CuBi2O4 heterostructures for persulfate-assisted photocatalytic degradation of dye contaminants under visible light. Journal of Photochemistry and Photobiology A: Chemistry, 2020, 391, 112397.	3.9	79
49	Novel g-C 3 N 4 /Ag 2 SO 4 nanocomposites: Fast microwave-assisted preparation and enhanced photocatalytic performance towards degradation of organic pollutants under visible light. Journal of Colloid and Interface Science, 2016, 482, 165-174.	9.4	76
50	Ternary magnetic g-C 3 N 4 /Fe 3 O 4 /Agl nanocomposites: Novel recyclable photocatalysts with enhanced activity in degradation of different pollutants under visible light. Materials Chemistry and Physics, 2016, 174, 59-69.	4.0	76
51	Integration of carbon dots and polyaniline with TiO2 nanoparticles: Substantially enhanced photocatalytic activity to removal various pollutants under visible light. Journal of Photochemistry and Photobiology A: Chemistry, 2018, 367, 94-104.	3.9	76
52	Facile preparation of novel quaternary g-C ₃ N ₄ /Fe ₃ O ₄ /AgI/Bi ₂ S ₃ nanocomposites: magnetically separable visible-light-driven photocatalysts with significantly enhanced activity. RSC Advances, 2016, 6, 106572-106583.	3.6	74
53	Bio-extract-mediated ZnO nanoparticles: microwave-assisted synthesis, characterization and antidiabetic activity evaluation. Artificial Cells, Nanomedicine and Biotechnology, 2018, 46, 730-739.	2.8	73
54	Graphitic Carbon Nitride/Chitosan Composite for Adsorption and Electrochemical Determination of Mercury in Real Samples. Industrial & Engineering Chemistry Research, 2016, 55, 8114-8122.	3.7	71

#	Article	IF	CITATIONS
55	Ag3VO4/ZnO nanocomposites with an n–n heterojunction as novel visible-light-driven photocatalysts with highly enhanced activity. Materials Science in Semiconductor Processing, 2015, 39, 671-679.	4.0	70
56	Facile preparation of Fe3O4@AgBr–ZnO nanocomposites as novel magnetically separable visible-light-driven photocatalysts. Ceramics International, 2015, 41, 1467-1476.	4.8	70
57	Fabrication of novel ZnO/BiOBr/C-Dots nanocomposites with considerable photocatalytic performances in removal of organic pollutants under visible light. Advanced Powder Technology, 2019, 30, 1197-1209.	4.1	69
58	Novel magnetically separable g-C3N4/Fe3O4/Ag3PO4/Co3O4 nanocomposites: Visible-light-driven photocatalysts with highly enhanced activity. Advanced Powder Technology, 2017, 28, 1540-1553.	4.1	68
59	Integration of Ag2WO4 and AgBr with TiO2 to fabricate ternary nanocomposites: Novel plasmonic photocatalysts with remarkable activity under visible light. Materials Research Bulletin, 2018, 99, 93-102.	5.2	68
60	Fabrication of novel g-C3N4 nanosheet/carbon dots/Ag6Si2O7 nanocomposites with high stability and enhanced visible-light photocatalytic activity. Journal of the Taiwan Institute of Chemical Engineers, 2019, 103, 94-109.	5.3	68
61	ZnO/ZnBi2O4 nanocomposites with p-n heterojunction as durable visible-light-activated photocatalysts for efficient removal of organic pollutants. Journal of Alloys and Compounds, 2020, 826, 154229.	5.5	68
62	Microwave-assisted preparation of Ce-doped ZnO nanostructures as an efficient photocatalyst. Materials Letters, 2013, 110, 53-56.	2.6	66
63	Decoration of Fe3O4 and CoWO4 nanoparticles over graphitic carbon nitride: Novel visible-light-responsive photocatalysts with exceptional photocatalytic performances. Materials Research Bulletin, 2018, 105, 159-171.	5.2	66
64	Green synthesis of ZnO and ZnO/CuO nanocomposites in Mentha longifolia leaf extract: characterization and their application as anti-bacterial agents. Journal of Materials Science: Materials in Electronics, 2018, 29, 13596-13605.	2.2	66
65	A novel ZrB2–C3N4 composite with improved mechanical properties. Ceramics International, 2019, 45, 21512-21519.	4.8	66
66	Graphitic carbon nitride nanosheets anchored with BiOBr and carbon dots: Exceptional visible-light-driven photocatalytic performances for oxidation and reduction reactions. Journal of Colloid and Interface Science, 2018, 530, 642-657.	9.4	65
67	Ternary g-C3N4/Fe3O4/Ag3VO4 nanocomposites: Novel magnetically separable visible-light-driven photocatalysts for efficiently degradation of dye pollutants. Materials Chemistry and Physics, 2015, 163, 421-430.	4.0	63
68	Fabrication of TiO2/CoMoO4/PANI nanocomposites with enhanced photocatalytic performances for removal of organic and inorganic pollutants under visible light. Materials Chemistry and Physics, 2019, 224, 10-21.	4.0	63
69	Ultrasonic-assisted preparation of novel ternary ZnO/AgI/Fe 3 O 4 nanocomposites as magnetically separable visible-light-driven photocatalysts with excellent activity. Journal of Colloid and Interface Science, 2016, 461, 144-153.	9.4	62
70	Integration of NiWO4 and Fe3O4 with graphitic carbon nitride to fabricate novel magnetically recoverable visible-light-driven photocatalysts. Journal of Materials Science, 2018, 53, 9046-9063.	3.7	62
71	Sol-gel/MOF nanocomposite for effective protection of 2024 aluminum alloy against corrosion. Surface and Coatings Technology, 2019, 380, 125038.	4.8	61
72	High performance magnetically recoverable g-C3N4/Fe3O4/Ag/Ag2SO3 plasmonic photocatalyst for enhanced photocatalytic degradation of water pollutants. Advanced Powder Technology, 2017, 28, 565-574.	4.1	60

#	Article	IF	CITATIONS
73	Synthesis and characterization of TiO2–graphene nanocomposites modified with noble metals as a photocatalyst for degradation of pollutants. Applied Catalysis A: General, 2013, 462-463, 82-90.	4.3	59
74	Synthesis of novel p-n-p BiOBr/ZnO/BiOI heterostructures and their efficient photocatalytic performances in removals of dye pollutants under visible light. Journal of Photochemistry and Photobiology A: Chemistry, 2020, 389, 112247.	3.9	59
75	Ternary ZnO/AgBr/Ag2CrO4 nanocomposites with tandem n–n heterojunctions as novel visible-light-driven photocatalysts with excellent activity. Ceramics International, 2015, 41, 14383-14393.	4.8	58
76	Improving visible-light-induced photocatalytic ability of TiO2 through coupling with Bi3O4Cl and carbon dot nanoparticles. Separation and Purification Technology, 2020, 238, 116404.	7.9	57
77	Novel ZnO/Ag2CrO4 nanocomposites with n–n heterojunctions as excellent photocatalysts for degradation of different pollutants under visible light. Journal of Materials Science: Materials in Electronics, 2016, 27, 4098-4108.	2.2	56
78	A facile ultrasonic-aided biosynthesis of ZnO nanoparticles using Vaccinium arctostaphylos L. leaf extract and its antidiabetic, antibacterial, and oxidative activity evaluation. Ultrasonics Sonochemistry, 2019, 55, 57-66.	8.2	55
79	Preparation of novel nanocomposites by deposition of Ag2WO4 and AgI over ZnO particles: Efficient plasmonic visible-light-driven photocatalysts through a cascade mechanism. Ceramics International, 2017, 43, 13447-13460.	4.8	53
80	Exceptional photocatalytic activity for g-C3N4 activated by H2O2 and integrated with Bi2S3 and Fe3O4 nanoparticles for removal of organic and inorganic pollutants. Advanced Powder Technology, 2019, 30, 524-537.	4.1	52
81	Oxidized fullerene/sol-gel nanocomposite for corrosion protection of AM60B magnesium alloy. Surface and Coatings Technology, 2020, 385, 125400.	4.8	52
82	Fabrication of novel ZnO/MnWO 4 nanocomposites with p - n heterojunction: Visible-light-induced photocatalysts with substantially improved activity and durability. Journal of Materials Science and Technology, 2018, 34, 1891-1901.	10.7	51
83	Facile one-pot method for preparation of AgI/ZnO nanocomposites as visible-light-driven photocatalysts with enhanced activities. Materials Science in Semiconductor Processing, 2015, 34, 74-81.	4.0	50
84	Electroless Ni-P/nano-WO3 coating and its mechanical and corrosion protection properties. Journal of Alloys and Compounds, 2018, 769, 149-160.	5.5	50
85	Carbon dots and Bi4O5Br2 adhered on TiO2 nanoparticles: Impressively boosted photocatalytic efficiency for removal of pollutants under visible light. Separation and Purification Technology, 2020, 250, 117179.	7.9	50
86	One-pot ultrasonic-assisted method for preparation of Ag/AgCl sensitized ZnO nanostructures as visible-light-driven photocatalysts. Solid State Sciences, 2015, 40, 111-120.	3.2	49
87	Fe3O4/ZnO/Ag3VO4/AgI nanocomposites: Quaternary magnetic photocatalysts with excellent activity in degradation of water pollutants under visible light. Separation and Purification Technology, 2016, 166, 63-72.	7.9	49
88	Application of ultrasonic irradiation method for preparation of ZnO nanostructures doped with Sb+3 ions as a highly efficient photocatalyst. Applied Surface Science, 2013, 276, 468-475.	6.1	48
89	Preparation of AgCl–ZnO nanocomposites as highly efficient visible-light photocatalysts in water by one-pot refluxing method. Journal of Alloys and Compounds, 2014, 601, 1-8.	5.5	47
90	Enriched zinc oxide nanoparticles by Nasturtium officinale leaf extract: Joint ultrasound-microwave-facilitated synthesis, characterization, and implementation for diabetes control and bacterial inhibition. Ultrasonics Sonochemistry, 2019, 58, 104613.	8.2	47

#	Article	IF	CITATIONS
91	Synthesis of novel AgCl loaded g-C3N5 with ultrahigh activity as visible light photocatalyst for pollutants degradation. Chemical Physics Letters, 2020, 738, 136862.	2.6	47
92	Application of principal component-genetic algorithm-artificial neural network for prediction acidity constant of various nitrogen-containing compounds in water. Monatshefte Für Chemie, 2009, 140, 15-27.	1.8	46
93	Application of artificial neural networks for predicting the aqueous acidity of various phenols using QSAR. Journal of Molecular Modeling, 2006, 12, 338-347.	1.8	45
94	A simple large-scale method for preparation of g-C ₃ N ₄ /SnO ₂ nanocomposite as visible-light-driven photocatalyst for degradation of an organic pollutant. Materials Express, 2015, 5, 309-318.	0.5	45
95	Photosensitization of Fe3O4/ZnO by AgBr and Ag3PO4 to fabricate novel magnetically recoverable nanocomposites with significantly enhanced photocatalytic activity under visible-light irradiation. Ceramics International, 2016, 42, 15224-15234.	4.8	45
96	Novel magnetic g-C3N4/Fe3O4/AgCl nanocomposites: Facile and large-scale preparation and highly efficient photocatalytic activities under visible-light irradiation. Materials Science in Semiconductor Processing, 2015, 39, 162-171.	4.0	44
97	High corrosion protection performance of the LDH/Ni-P composite coating on AM60B magnesium alloy. Surface and Coatings Technology, 2020, 397, 125979.	4.8	44
98	Visible-light photosensitization of ZnO by Bi2MoO6 and AgBr: Role of tandem n-n heterojunctions in efficient charge transfer and photocatalytic performances. Materials Chemistry and Physics, 2018, 214, 107-119.	4.0	43
99	Synergistic antidiabetic activity of ZnO nanoparticles encompassed by Urtica dioica extract. Advanced Powder Technology, 2020, 31, 2110-2118.	4.1	43
100	Synthesis of novel ternary g-C3N4/SiC/C-Dots photocatalysts and their visible-light-induced activities in removal of various contaminants. Journal of Photochemistry and Photobiology A: Chemistry, 2020, 392, 112431.	3.9	43
101	Comparison between preparative methodologies of nanostructured carbon nitride and their use as selective photocatalysts in water suspension. Research on Chemical Intermediates, 2017, 43, 5153-5168.	2.7	42
102	Ultrasonic-assisted preparation of novel ternary ZnO/AgI/Ag2CrO4 nanocomposites as visible-light-driven photocatalysts with excellent activity. Materials Science in Semiconductor Processing, 2016, 44, 48-56.	4.0	41
103	Boosted visible-light photocatalytic performance of TiO2-x decorated by BiOI and AgBr nanoparticles. Journal of Photochemistry and Photobiology A: Chemistry, 2019, 384, 112066.	3.9	41
104	Ternary ZnO/AgI/Ag2CO3 nanocomposites: Novel visible-light-driven photocatalysts with excellent activity in degradation of different water pollutants. Materials Chemistry and Physics, 2016, 184, 210-221.	4.0	40
105	Enhanced anti-bacterial activities of ZnO nanoparticles and ZnO/CuO nanocomposites synthesized using Vaccinium arctostaphylos L. fruit extract. Artificial Cells, Nanomedicine and Biotechnology, 2018, 46, 1200-1209.	2.8	40
106	One-pot hydrothermal synthesis of CuCo2S4/RGO nanocomposites for visible-light photocatalytic applications. Journal of Physics and Chemistry of Solids, 2018, 123, 242-253.	4.0	39
107	Oxygen-rich TiO2 decorated with C-Dots: Highly efficient visible-light-responsive photocatalysts in degradations of different contaminants. Advanced Powder Technology, 2019, 30, 1183-1196.	4.1	39
108	BiOBr and BiOCl decorated on TiO2 QDs: Impressively increased photocatalytic performance for the degradation of pollutants under visible light. Advanced Powder Technology, 2020, 31, 3582-3596.	4.1	39

#	Article	IF	CITATIONS
109	TiO2/CDs modified thin-film nanocomposite polyamide membrane for simultaneous enhancement of antifouling and chlorine-resistance performance. Desalination, 2022, 525, 115506.	8.2	39
110	Photosensitization of ZnO with Ag 3 VO 4 and AgI nanoparticles: Novel ternary visible-light-driven photocatalysts with highly enhanced activity. Advanced Powder Technology, 2016, 27, 1427-1437.	4.1	38
111	Electrochemical noise analysis to examine the corrosion behavior of Ni-P deposit on AM60B alloy plated by Zr pretreatment. Surface and Coatings Technology, 2018, 346, 29-39.	4.8	38
112	Ni, Pd, and Pt-embedded graphitic carbon nitrides as excellent adsorbents for HCN removal: A DFT study. Applied Surface Science, 2018, 456, 882-889.	6.1	38
113	Visible-light-activated g-C3N4 nanosheet/carbon dot/FeOCl nanocomposites: Photodegradation of dye pollutants and tetracycline hydrochloride. Colloids and Surfaces A: Physicochemical and Engineering Aspects, 2021, 617, 126424.	4.7	38
114	Sol-gel coating filled with SDS-stabilized fullerene nanoparticles for active corrosion protection of the magnesium alloy. Surface and Coatings Technology, 2021, 419, 127292.	4.8	38
115	Biomolecule-assisted solvothermal synthesis of Cu ₂ SnS ₃ flowers/RGO nanocomposites and their visible-light-driven photocatalytic activities. RSC Advances, 2016, 6, 74177-74185.	3.6	36
116	Combining carbon dots and Ag6Si2O7 nanoparticles with TiO2: Visible-light-driven photocatalysts with efficient performance for removal of pollutants. Separation and Purification Technology, 2020, 248, 116928.	7.9	36
117	Anchoring Bi4O5I2 and AgI nanoparticles over g-C3N4 nanosheets: Impressive visible-light-induced photocatalysts in elimination of hazardous contaminates by a cascade mechanism. Advanced Powder Technology, 2020, 31, 2618-2628.	4.1	36
118	Integration of Bi4O5I2 nanoparticles with ZnO: Impressive visible-light-induced systems for elimination of aqueous contaminants. Journal of the Taiwan Institute of Chemical Engineers, 2021, 119, 177-186.	5.3	36
119	Hydrothermal low-temperature preparation and characterization of ZnO nanoparticles supported on natural zeolite as a highly efficient photocatalyst. Monatshefte FÃ1⁄4r Chemie, 2011, 142, 119-129.	1.8	35
120	Ultrasonic-assisted one-pot preparation of ZnO/Ag3VO4 nanocomposites for efficiently degradation of organic pollutants under visible-light irradiation. Solid State Sciences, 2015, 49, 68-77.	3.2	35
121	Novel magnetically separable Fe 3 O 4 @ZnO/AgCl nanocomposites with highly enhanced photocatalytic activities under visible-light irradiation. Separation and Purification Technology, 2015, 147, 194-202.	7.9	34
122	A first-principle investigation of NO2 adsorption behavior on Co, Rh, and Ir-embedded graphitic carbon nitride: Looking for highly sensitive gas sensor. Physics Letters, Section A: General, Atomic and Solid State Physics, 2020, 384, 126057.	2.1	34
123	Hydrogen peroxide treated g-C3N4 as an effective hydrophilic nanosheet for modification of polyethersulfone membranes with enhanced permeability and antifouling characteristics. Chemosphere, 2021, 279, 130616.	8.2	34
124	Kinetics study of a Dielsâ€Alder reaction in mixtures of an ionic liquid with molecular solvents. Journal of Physical Organic Chemistry, 2008, 21, 783-788.	1.9	33
125	Ultrasound-assisted preparation and characterization of β-Bi2O3 nanostructures: Exploring the photocatalytic activity against rhodamine B. Superlattices and Microstructures, 2015, 81, 151-160.	3.1	33
126	Codeposition of AgI and Ag2CrO4 on g-C3N4/Fe3O4 nanocomposite: Novel magnetically separable visible-light-driven photocatalysts with enhanced activity. Advanced Powder Technology, 2016, 27, 2496-2506.	4.1	33

#	Article	IF	CITATIONS
127	Integration of BiOI and Ag3PO4 nanoparticles onto oxygen vacancy rich-TiO2 for efficient visible-light photocatalytic decontaminations. Journal of Photochemistry and Photobiology A: Chemistry, 2020, 400, 112659.	3.9	33
128	Prediction of basicity constants of various pyridines in aqueous solution using a principal component-genetic algorithm-artificial neural network. Monatshefte Für Chemie, 2008, 139, 1423-1431.	1.8	32
129	Novel ternary g-C3N4/Ag3VO4/AgBr nanocomposites with excellent visible-light-driven photocatalytic performance for environmental applications. Solid State Sciences, 2018, 78, 133-143.	3.2	32
130	Novel ZnO/Ag6Si2O7 nanocomposites for activation of persulfate ions in photocatalytic removal of organic contaminants under visible light. Materials Chemistry and Physics, 2020, 239, 121988.	4.0	32
131	Effect of operational parameters on photodegradation of methylene blue on ZnS nanoparticles prepared in presence of an ionic liquid as a highly efficient photocatalyst. Journal of the Iranian Chemical Society, 2011, 8, S169-S175.	2.2	31
132	Microwave-assisted method for preparation of Zn1â^'xMgxO nanostructures and their activities for photodegradation of methylene blue. Advanced Powder Technology, 2014, 25, 1016-1025.	4.1	31
133	Ternary ZnO/Ag3VO4/Fe3O4 nanocomposites: Novel magnetically separable photocatalyst for efficiently degradation of dye pollutants under visible-light irradiation. Solid State Sciences, 2015, 48, 177-185.	3.2	31
134	Synthesis of magnetically recoverable visible-light-induced photocatalysts by combination of Fe3O4/ZnO with BiOI and polyaniline. Progress in Natural Science: Materials International, 2019, 29, 145-155.	4.4	31
135	Template-free preparation and characterization of nanocrystalline ZnO in aqueous solution of [EMIM][EtSO4] as a low-cost ionic liquid using ultrasonic irradiation and photocatalytic activity. Journal of Physics and Chemistry of Solids, 2009, 70, 1353-1358.	4.0	30
136	Graphitic carbon nitride (g-C3N4/Fe3O4/BiOI)-carbon composite electrode as a highly sensitive and selective citric acid sensor: Three-component nanocomposite as a definitive factor for selectivity in catalysis. Sensors and Actuators B: Chemical, 2019, 279, 245-254.	7.8	30
137	Efficiently enhanced nitrogen fixation performance of g-C3N4 nanosheets by decorating Ni3V2O8 nanoparticles under visible-light irradiation. Ceramics International, 2020, 46, 24472-24482.	4.8	30
138	Solvatochromic parameters for binary mixtures of an ionic liquid with various protic molecular solvents. Monatshefte Für Chemie, 2009, 140, 329-334.	1.8	28
139	Solvent effects on the reaction rate and selectivity of synchronous heterogeneous hydrogenation of cyclohexene and acetone in ionic liquid/alcohols mixtures. Journal of Molecular Catalysis A, 2009, 306, 11-16.	4.8	28
140	Antifungal activity of magnetically separable Fe3O4/ZnO/AgBr nanocomposites prepared by a facile microwave-assisted method. Progress in Natural Science: Materials International, 2016, 26, 334-340.	4.4	28
141	ZnO/Ag/Ag ₂ WO ₄ photo-electrodes with plasmonic behavior for enhanced photoelectrochemical water oxidation. RSC Advances, 2019, 9, 8271-8279.	3.6	28
142	Novel ZnO/Ag3PO4/AgI photocatalysts: Preparation, characterization, and the excellent visible-light photocatalytic performances. Materials Science in Semiconductor Processing, 2020, 119, 105229.	4.0	28
143	Nanodiamond incorporated solâ~gel coating for corrosion protection of magnesium alloy. Transactions of Nonferrous Metals Society of China, 2020, 30, 1535-1549.	4.2	28
144	Preparation and characterization of monodispersed nanocrystalline ZnS in water-rich [EMIM]EtSO4 ionic liquid using ultrasonic irradiation. Journal of Crystal Growth, 2008, 310, 4544-4548.	1.5	27

#	Article	IF	CITATIONS
145	Microwave-assisted preparation and characterization of Zn1â^'xCdxS nanoparticles in presence of an ionic liquid and their photocatalytic activities. Journal of Alloys and Compounds, 2010, 496, 650-655.	5.5	27
146	Adsorption performance of SO2 gases over the transition metal/P‒codoped graphitic carbon nitride: A DFT investigation. Materials Chemistry and Physics, 2020, 243, 122602.	4.0	27
147	Graphitic carbon nitride as a fascinating adsorbent for toxic gases: A mini-review. Chemical Physics Letters, 2020, 754, 137676.	2.6	27
148	Solvent effects on kinetics of the reaction between 2â€chloroâ€3,5â€dinitropyridine and aniline in aqueous and alcoholic solutions of [bmim]BF ₄ . International Journal of Chemical Kinetics, 2007, 39, 681-687.	1.6	26
149	Preparation and characterization of SnO2 nanoparticles in aqueous solution of [EMIM][EtSO4] as a low cost ionic liquid using ultrasonic irradiation. Powder Technology, 2009, 195, 63-67.	4.2	26
150	Competitive Adsorption of Methylene Blue and Rhodamine B on Natural Zeolite: Thermodynamic and Kinetic Studies. Chinese Journal of Chemistry, 2010, 28, 349-356.	4.9	26
151	Remarkable improvement in hydrogen storage capabilities of graphitic carbon nitride nanosheets under selected transition metal embedding: A DFT study. International Journal of Hydrogen Energy, 2021, 46, 33864-33876.	7.1	26
152	Spin regulation on (Co,Ni)Se2/C@FeOOH hollow nanocage accelerates water oxidation. Chinese Journal of Catalysis, 2022, 43, 839-850.	14.0	26
153	Ultrasonic-assisted preparation and characterization of CdS nanoparticles in the presence of a halide-free and low-cost ionic liquid and photocatalytic activity. Journal of Physics and Chemistry of Solids, 2010, 71, 1393-1397.	4.0	25
154	n–n ZnO–Ag ₂ CrO ₄ heterojunction photoelectrodes with enhanced visible-light photoelectrochemical properties. RSC Advances, 2019, 9, 7992-8001.	3.6	25
155	Application of a genetic algorithm and an artificial neural network for global prediction of the toxicity of phenols to Tetrahymena pyriformis. Monatshefte Für Chemie, 2009, 140, 1279-1288.	1.8	24
156	Pretreatment-free Niâ^'P plating on magnesium alloy at low temperatures. Transactions of Nonferrous Metals Society of China, 2018, 28, 2478-2488.	4.2	24
157	Fe, Ru, and Os‒embedded graphitic carbon nitride as a promising candidate for NO gas sensor: A first-principles investigation. Materials Chemistry and Physics, 2019, 231, 264-271.	4.0	24
158	Kinetic study of heterogeneous catalytic hydrogenation of cyclohexene to cyclohexane in ionic liquid–alcohols mixtures. Applied Catalysis A: General, 2008, 341, 58-64.	4.3	23
159	Novel magnetically separable g-C3N4/Fe3O4/Ag3VO4/Ag2CrO4 nanocomposites as efficient visible-light-driven photocatalysts for degradation of water pollutants. Journal of Materials Science: Materials in Electronics, 2016, 27, 8532-8545.	2.2	23
160	Ultrasonic-assisted preparation of novel ternary ZnO/Ag 3 VO 4 /Ag 2 CrO 4 nanocomposites and their enhanced visible-light activities in degradation of different pollutants. Solid State Sciences, 2016, 55, 58-68.	3.2	23
161	Preparation of novel ternary TiO2 QDs/CDs/AgI nanocomposites with superior visible-light induced photocatalytic activity. Journal of Photochemistry and Photobiology A: Chemistry, 2019, 385, 112070.	3.9	23
162	Preparation and characterization of ZnO nanocrystallines in the presence of an ionic liquid using microwave irradiation and photocatalytic activity. Journal of the Iranian Chemical Society, 2010, 7, S70-S82.	2.2	22

#	Article	IF	CITATIONS
163	Preparation of Ag/ZnMgO nanocomposites as novel highly efficient photocatalysts by one-pot method under microwave irradiation. Journal of Photochemistry and Photobiology A: Chemistry, 2014, 281, 59-67.	3.9	22
164	Novel ternary g-C3N4 nanosheet/Ag2MoO4/AgI photocatalysts: Impressive photocatalysts for removal of various contaminants. Journal of Photochemistry and Photobiology A: Chemistry, 2020, 403, 112871.	3.9	22
165	Novel visible-light-driven photocatalyst of NiO/Cd/g-C3N4 for enhanced degradation of methylene blue. Arabian Journal of Chemistry, 2020, 13, 5810-5820.	4.9	22
166	Integration g-C3N4 nanotubes and Sb2MoO6 nanoparticles: Impressive photoactivity for tetracycline degradation, Cr (VI) reduction, and organic dyes removals under visible light. Advanced Powder Technology, 2021, 32, 2322-2335.	4.1	22
167	Facile Solvothermal Synthesis of Novel CuCo2S4/g-C3N4 Nanocomposites for Visible-Light Photocatalytic Applications. Journal of Inorganic and Organometallic Polymers and Materials, 2018, 28, 1276-1285.	3.7	21
168	Photocatalytic performance of oxygen vacancy rich-TiO2 combined with Bi4O5Br2 nanoparticles on degradation of several water pollutants. Advanced Powder Technology, 2021, 32, 304-316.	4.1	21
169	Nanoarchitecturing TiO2/NiCr2O4 p-n heterojunction photocatalysts for visible-light-induced activation of persulfate to remove tetracycline hydrochloride. Chemosphere, 2022, 300, 134594.	8.2	21
170	Hydrothermal and template-free preparation and characterization of nanocrystalline ZnS in presence of a low-cost ionic liquid and photocatalytic activity. Physica E: Low-Dimensional Systems and Nanostructures, 2010, 42, 1973-1978.	2.7	20
171	Microwaveâ€assisted synthesis of the <scp>Fe₂O₃</scp> / <scp>gâ€C₃N₄</scp> nanocomposites with enhanced photocatalytic activity for degradation of methylene blue. Journal of the Chinese Chemical Society. 2020. 67, 2032-2041.	1.4	20
172	Combination of CoWO 4 and Ag 3 VO 4 with Fe 3 O 4 /ZnO nanocomposites: Magnetic photocatalysts with enhanced activity through p-n-n heterojunctions under visible light. Solid State Sciences, 2017, 74, 24-36.	3.2	19
173	Biologicallyâ€synthesised ZnO/CuO/Ag nanocomposite using propolis extract and coated on the gauze for wound healing applications. IET Nanobiotechnology, 2020, 14, 548-554.	3.8	19
174	Integration of oxygen vacancy rich-TiO2 with BiOI and Ag6Si2O7: Ternary p-n-n photocatalysts with greatly increased performances for degradation of organic contaminants. Colloids and Surfaces A: Physicochemical and Engineering Aspects, 2021, 613, 126101.	4.7	19
175	Visible-light-triggered persulfate activation by CuCo2S4 modified ZnO photocatalyst for degradation of tetracycline hydrochloride. Colloids and Surfaces A: Physicochemical and Engineering Aspects, 2022, 642, 128640.	4.7	19
176	Combining brown titanium dioxide with BiOBr and AgBr nanoparticles using a facile one-pot procedure to promote visible-light photocatalytic performance. Journal of Photochemistry and Photobiology A: Chemistry, 2022, 431, 114034.	3.9	19
177	Prediction dielectric constant of different ternary liquid mixtures at various temperatures and compositions using artificial neural networks. Physics and Chemistry of Liquids, 2007, 45, 471-478.	1.2	18
178	Solvent effects on kinetics of an aromatic nucleophilic substitution reaction in mixtures of an ionic liquid with molecular solvents and prediction using artificial neural networks. International Journal of Chemical Kinetics, 2009, 41, 153-159.	1.6	18
179	Simple and low temperature preparation and characterization of CdS nanoparticles as a highly efficient photocatalyst in presence of a low-cost ionic liquid. Journal of the Iranian Chemical Society, 2010, 7, S175-S186.	2.2	18
180	Microwave-assisted facile one-pot method for preparation of BiOl–ZnO nanocomposites as novel dye adsorbents by synergistic collaboration. Journal of the Iranian Chemical Society, 2015, 12, 909-919.	2.2	18

#	Article	IF	CITATIONS
181	Adsorption and photocatalytic degradation of methylene blue on Zn1â^'xCuxS nanoparticles prepared by a simple green method. Applied Surface Science, 2011, 257, 2361-2366.	6.1	17
182	Microwaveâ€assisted preparation of nanocrystalline ZnS in aqueous solutions of [EMIM][EtSO ₄] as a lowâ€cost ionic liquid, and its characterization and photocatalytic properties. Physica Status Solidi (A) Applications and Materials Science, 2009, 206, 2529-2535.	1.8	16
183	Microwave-assisted method for preparation of Sb-doped ZnO nanostructures and their photocatalytic activity. Journal of the Iranian Chemical Society, 2014, 11, 457-465.	2.2	16
184	Combination of Ag 2 CrO 4 and AgI semiconductors with g-C 3 N 4 : Novel nanocomposites with substantially improved photocatalytic performance under visible light. Solid State Sciences, 2018, 77, 62-73.	3.2	16
185	Activation of persulfate ions by TiO2/carbon dots nanocomposite under visible light for photocatalytic degradations of organic contaminants. Journal of Materials Science: Materials in Electronics, 2019, 30, 12510-12522.	2.2	16
186	Prediction of normalized polarity parameter in binary mixed solvent systems using artificial neural networks. Physics and Chemistry of Liquids, 2005, 43, 239-247.	1.2	15
187	Microwave-Assisted Preparation of CdS Nanoparticles in a Halide-Free Ionic Liquid and Their Photocatalytic Activities. Chinese Journal of Catalysis, 2011, 32, 933-938.	14.0	15
188	Heterogeneous photocatalytic activation of persulfate ions with novel ZnO/AgFeO2 nanocomposite for contaminants degradation under visible light. Journal of Materials Science: Materials in Electronics, 2021, 32, 4272-4289.	2.2	15
189	C-C3N4 nanosheets adhered with Ag3BiO3 and carbon dots with appreciably promoted photoactivity towards elimination of several contaminants. Advanced Powder Technology, 2021, 32, 1196-1206.	4.1	15
190	Impressive visible-light photocatalytic performance of TiO2 by integration with Bi2SiO5 nanoparticles: Binary TiO2/Bi2SiO5 photocatalysts with n-n heterojunction. Colloids and Surfaces A: Physicochemical and Engineering Aspects, 2021, 629, 127392.Cockmunication	4.7	15
191	xmins:mml= http://www.w3.org/1998/Math/Math/MathML_display= inline_id= d1e418 altimg="sil1.svg"> <mml:msub><mml:mrow /><mml:mrow><mml:mn>2</mml:mn></mml:mrow></mml:mrow </mml:msub> O <mml:math xmlns:mml="http://www.w3.org/1998/Math/MathML" display="inline" id="d1e426"</mml:math 	6.1	15
192	Sonochemical preparation of AgBr–ZnO nanocomposites in water using one-pot method as highly efficient photocatalysts under visible light. Journal of the Iranian Chemical Society, 2015, 12, 1961-1971.	2.2	14
193	A first-principles study on the interaction of CO molecules with VIII transition metals-embedded graphitic carbon nitride as an excellent candidate for CO sensor. Physics Letters, Section A: General, Atomic and Solid State Physics, 2019, 383, 2472-2480.	2.1	14
194	Synergistic Coupling of NiTe Nanoarrays with FeOOH Nanosheets for Highly Efficient Oxygen Evolution Reaction. ChemElectroChem, 2021, 8, 3643-3650.	3.4	14
195	Fast, green and template-free method for preparation of Zn1â^'xCdxS nanoparticles using microwave irradiation and their photocatalytic activities. Physica E: Low-Dimensional Systems and Nanostructures, 2010, 43, 216-223.	2.7	13
196	Co-regulative effects of chitosan-fennel seed extract system on the hormonal and biochemical factors involved in the polycystic ovarian syndrome. Materials Science and Engineering C, 2020, 117, 111351.	7.3	12
197	Microwave-assisted preparation of Znlâ [^] xCuxS nanoparticles by a fast, green, and template-free method and photocatalytic activity. Desalination, 2011, 271, 273-278.	8.2	11
198	Adsorption of HCN molecules on Ni, Pd and Pt-doped (7, 0) boron nitride nanotube: a DFT study. Molecular Physics, 2018, 116, 1320-1327.	1.7	11

#	Article	IF	CITATIONS
199	Combination of NiWO4 and polyaniline with TiO2: fabrication of ternary photocatalysts with highly visible-light-induced photocatalytic performances. Journal of the Iranian Chemical Society, 2020, 17, 351-365.	2.2	11
200	A DFT study for adsorption of CO on Ni, Pd and Pt atoms doped (7, 0) boron nitride nanotube. Molecular Physics, 2018, 116, 204-211.	1.7	10
201	Pâ€doped <scp>gâ€C₃N₄</scp> as an efficient photocatalyst for <scp>CO₂</scp> conversion into valueâ€added materials: a joint experimental and theoretical study. International Journal of Quantum Chemistry, 2020, 120, e26388.	2.0	10
202	Integration of Bi5O7I with TiO2: Binary photocatalysts with boosted visible-light photocatalysis in removal of organic contaminants. Journal of Photochemistry and Photobiology A: Chemistry, 2021, 410, 113190.	3.9	10
203	Fabrication of TiO2/CeO2/CeFeO3 tandem n-n heterojunction nanocomposites for visible-light-triggered photocatalytic degradation of tetracycline and colored effluents. Ceramics International, 2022, 48, 22352-22361.	4.8	10
204	Binary visible-light-triggered ZnO/Bi4O5Br2 photocatalysts with n-n heterojunction: Simple fabrication and impressively activation of peroxodisulfate ions for degradation of tetracycline. Surfaces and Interfaces, 2022, 32, 102147.	3.0	9
205	QSAR study of the 5-HT1A receptor affinities of arylpiperazines using a genetic algorithm–artificial neural network model. Monatshefte Für Chemie, 2009, 140, 523-530.	1.8	8
206	Facile ultrasonic-assisted preparation of Fe3O4/Ag3VO4 nanocomposites as magnetically recoverable visible-light-driven photocatalysts with considerable activity. Journal of the Iranian Chemical Society, 2017, 14, 863-872.	2.2	8
207	Biogenic integrated ZnO/Ag nanocomposite: Surface analysis and in vivo practices for the management of type 1 diabetes complications. Colloids and Surfaces B: Biointerfaces, 2020, 189, 110878.	5.0	8
208	Novel ZnO/CuBiS2 nanocomposites with p-n heterojunctions for persulfate-promoted photocatalytic mitigation of pollutants under visible light. Surfaces and Interfaces, 2021, 27, 101518.	3.0	8
209	Novel visible-light TiO2/Bi3O4Br photocatalysts with n-n heterojunction: Highly impressive performance for elimination of tetracycline and dye contaminants. Optical Materials, 2022, 123, 111831.	3.6	8
210	Facile fabrication of TiO ₂ /Bi ₅ O ₇ Br photocatalysts for visible-light-assisted removal of tetracycline and dye wastewaters. Journal Physics D: Applied Physics, 2022, 55, 165105.	2.8	8
211	Preparation of Cd(OH)2 nanostructures in water using a simple refluxing method and their photocatalytic activity. Journal of the Iranian Chemical Society, 2012, 9, 163-169.	2.2	7
212	Antifungal activity of TiO ₂ /AgBr nanocomposites on some phytopathogenic fungi. Food Science and Nutrition, 2021, 9, 3815-3823.	3.4	7
213	Preparation of Zn _{1–} <i> _x </i> Mn <i> _x </i> O nanoparticles by a simple "green―method and photocatalytic activity under visible light irradiation. International Journal of Materials Research, 2011, 102, 1397-1402.	0.3	6
214	Microwave-assisted one-pot preparation of AgBr/ZnO nanocomposites as highly efficient visible-light photocatalyst for inactivation of <i>Escherichia coli</i> . Materials Express, 2015, 5, 201-210.	0.5	6
215	Polyethylene glycol-doped BiZn ₂ VO ₆ as a high-efficiency solar-light-activated photocatalyst with substantial durability toward photodegradation of organic contaminations. RSC Advances, 2018, 8, 37480-37491.	3.6	6
216	DFT investigation for NH3 adsorption behavior on Fe, Ru, and Os-embedded graphitic carbon nitride: promising candidates for ammonia adsorbent. Journal of the Iranian Chemical Society, 2020, 17, 25-35.	2.2	6

#	Article	IF	CITATIONS
217	Integration of C-dots with g-C3N4 nanosheet/Ag2CO3 nanocomposites as effective Z-scheme visible-light photocatalysts for removal of hazardous organic and inorganic contaminates. Journal of Materials Science: Materials in Electronics, 2020, 31, 13392-13407.	2.2	6
218	Adsorption behavior of H2S on P‒doped, V/P, Nb/P, and Ta/P‒codoped graphitic carbon nitride: A first-principles investigation. Materials Chemistry and Physics, 2020, 252, 123117.	4.0	6
219	Synergistic influence of SiC and C ₃ N ₄ reinforcements on the characteristics of ZrB ₂ -based composites. Journal of Asian Ceramic Societies, 2021, 9, 53-62.	2.3	6
220	Fabrication, characterization, and photocatalytic studies of novel ZnO/Ag3BiO3 nanocomposites: impressive photocatalysts for degradation of some dyes. Journal of Materials Science: Materials in Electronics, 2021, 32, 2704-2718.	2.2	6
221	Enhancing photocatalytic activity of ZnO nanostructures by doping with Ce ⁺⁴ ions prepared in water using ultrasonic irradiation. International Journal of Materials Research, 2014, 105, 288-295.	0.3	5
222	Microwave-assisted one-pot method for preparation of ZnO/AgI nanocomposites with highly enhanced photocatalytic activity under visible-light irradiation. Desalination and Water Treatment, 2016, 57, 16015-16023.	1.0	5
223	Online evaluation of electroless deposition rate by electrochemical noise method. Transactions of Nonferrous Metals Society of China, 2019, 29, 1753-1762.	4.2	5
224	Novel high-performance H2Se sensor based on Zn/P-, Cd/P-, and Hg/P-modified graphitic carbon nitride sheets: A DFT study. Journal of the Iranian Chemical Society, 2021, 18, 2447-2455.	2.2	4
225	A first-principles investigation of PH3 gas adsorption on the graphitic carbon nitride sheets modified with V/P, Nb/P, and Ta/P elements. Materials Chemistry and Physics, 2021, 269, 124282.	4.0	4
226	Antifungal Activities of Pure and ZnO-Encapsulated Essential Oil of Zataria multiflora on Alternaria solani as the Pathogenic Agent of Tomato Early Blight Disease. Frontiers in Plant Science, 0, 13, .	3.6	4
227	Application of PCâ€ANN to Acidity Constant Prediction of Various Phenols and Benzoic Acids in Water. Chinese Journal of Chemistry, 2008, 26, 875-885.	4.9	3
228	Ultrasonic-assisted decoration of Ag2WO4, AgI, and Ag nanoparticles over tubular g-C3N4: Plasmonic photocatalysts for impressive removal of tetracycline under visible light. Photochemical and Photobiological Sciences, 2022, 21, 1201-1215.	2.9	3
229	Enhancement in hydrogen storage capabilities of Cr, Mo, and W-embedded graphitic carbon nitride nanosheets: A DFT investigation. Chemical Physics Letters, 2022, 794, 139490.	2.6	3
230	Z-scheme-based heterostructure photocatalysts for organic pollutant degradation. , 2021, , 177-217.		2
231	Simple and template-free method for preparation of (ZnO)1â^x[Cd(OH)2]xnanoparticles in water and their photocatalytic activities. Environmental Technology (United Kingdom), 2011, 32, 1735-1741.	2.2	1
232	Simple ionic-liquid assisted method for preparation of Cd1-x Zn x S nanoparticles with improved photocatalytic activity. International Journal of Materials Research, 2012, 103, 1522-1527.	0.3	1
233	Electronic structure of ZnO(0001)/AgBr(111) heterojunction interface based on the TB-mBJ approximation. European Physical Journal B, 2018, 91, 1.	1.5	1
234	Antiproliferative activity of zinc oxide-silver nanocomposite interlinked with Vaccinium arctostaphylos L. fruit extract against cancer cells and bacteria. Chemical Papers, 2022, 76, 247-257.	2.2	1